Weierstraß-Institut
für Angewandte Analysis und Stochastik

im Forschungsverbund Berlin e.V.

Preprint ISSN 0946 – 8633

Effects of nonlocal feedback on traveling fronts in neural fields subject to transmission delay

A. Hutt[1]

submitted: 02 July 2004

[1] E-Mail: hutt@wias-berlin.de

No. 953
Berlin 2004

2000 *Mathematics Subject Classification.* 45J05 92C20.

Key words and phrases. nonlocal neural activity, traveling wave front, constant feedback delay.

A.Hutt is supported by DFG Research Center M̈athematics for key technologies: Modelling, simulation and optimization of real-world processes ¨.

Edited by
Weierstraß-Institut für Angewandte Analysis und Stochastik (WIAS)
Mohrenstraße 39
10117 Berlin
Germany

Fax: + 49 30 2044975
E-Mail: preprint@wias-berlin.de
World Wide Web: http://www.wias-berlin.de/

Abstract

The work introduces a model for reciprocal connections in neural fields by a nonlocal feedback mechanism, while the neural field exhibits nonlocal interactions and intra-areal transmission delays. We study the speed of traveling fronts with respect to the transmission delay, the spatial feedback range and the feedback delay for general axonal and feedback connectivity kernels. In addition, we find a novel shape of traveling fronts due to the applied feedback and criteria for its occurence are derived.

In recent years, propagating activity in spatially extended systems has been found experimentally in neural systems [20, 17, 4, 31, 35], in chemistry and biology [25, 24, 21]. In particular traveling fronts have attracted much interest in theory [26, 28, 8, 27, 24] partly due to experimental findings [33, 12, 15]. Several studies dealing with these phenomena treat the examined system by partial differential equations, which account for short-range spatial interactions. However, neural systems might exhibit long-range interactions by their underlying spatial structure [1]. This structure originates from dendritic arborizations of neurons and from spread of axonal connections. Hence, realistic models of neural activity have to treat nonlocal interactions by integrating kernels. These kernels reflect the underlying connectivity in neural tissue. However, connectivity kernels are known only for few functional areas as the visual cortex [22], the cerebellum [29] or the prefrontal cortex [23]. Thus, modeling of traveling phenomena in general neural systems necessitates the treatment for more general kernel types. We mention previous studies on the stability of neural fields for general homogeneous kernels [2, 14, 5]. The present work follows this idea in order to gain a classification scheme for traveling fronts. This letter is similar to previous studies considering general kernels [8, 28] or general synaptic responses [9], but contrasts to these studies by considering constant nonlocal feedback delay. The latter has been found experimentally in reciprocal-connected neural areas [32, 7] and plays a decisive role in neural information processing [30]. We shall show how the front speed depends on both additional delays and how the typical front shape changes by the feedback delay.

The conduction-based model [34, 13, 19] assumes neural populations coupled on a microscopic spatial level by chemical synapses. That is population ensembles represent a coarse-grained spatial field. In addition, the neural activity is expressed by dendritic currents and firing rates averaged over an ensemble entity. This assumption neglects single-spike activity and temporal coding of neurons, i.e. the neural firing times are uncorrelated [16]. Thus the model considers time-averaged spiking activity, i.e. coarse-grained temporal activity. By virtue of its mesoscopic spatial

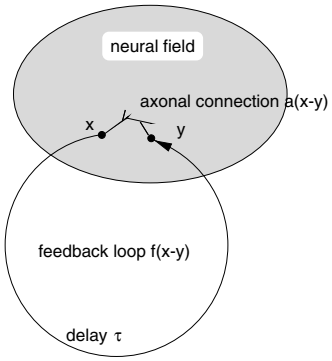

Figure 1: Sketch of intra-areal axonal connections and nonlocal feedback connections.

scale, such neural activity is recorded in neurophysiological experiments as local field potentials(e.g. [11]). In mathematical terms, the neural field is assumed being continous in space and time. The dendritic current V at location x at time t represents the linear delayed response of chemical synapses subject to incoming pulse activity. In turn, this pulse activity originates at a spatial location y by conversion from dendritic currents $V(y, t - \alpha(x, y))$. Here $\alpha(x, y)$ represents the delay time between origin and termination of the pulse. The present work treats two types of delay (Fig. 1). One type considers pulse activity propagating along axonal connections in the field and terminating at chemical synapses. This work focus to intracortical fields, which exhibit the same transmission speed v for both excitatory and inhibiory connections. Hence, the transmission delay is $\alpha(x, y) = |x-y|/v$. Further a nonlocal feedback loop is present with $\alpha(x, y) = \tau$, which terminates at either excitatory or inhibitory chemical synapses. We point out that both transmission and feedback delay are assumed homogeneous, i.e. the corresponding connectivity between two locations depends on their spatial distance only.

The model assumes a single time scale in the synaptic delay, which is set to unity by an appropriate time scaling. Hence, the dendritic current obeys

$$\frac{\partial}{\partial t}V(x,t) \;=\; -V(x,t) + a(x,t) + f(x,t) \tag{1}$$

$$a(x,t) = \int_{-\infty}^{\infty} A(x-y)S(V(y,t-|x-y|/v))\,dy$$

$$f(x,t) = \int_{-\infty}^{\infty} F(x-y)S(V(y,t-\tau))\,dy.$$

The functions $a(x, t)$ and $f(x, t)$ represent the synaptic input by axonal and feedback connections, respectively. The corresponding connectivity functions $A(x)$ and $F(x)$ are introduced as probability density functions of connections, i.e. $\int_{-\infty}^{\infty} A(x)dx = \kappa < \infty$, $\int_{-\infty}^{\infty} F(x)dx = \mu < \infty$. Here, the constants κ and μ represent the synaptic

strength of axonal and nonlocal feedback contributions, respectively. The axonal transmission speed v and the constant feedback delay τ introduce two more time scales to the system, in addition to the synaptic delay. The conversion from dendritic currents to pulse rates is given by the transfer function S. It reflects the statistical properties of firing thresholds and active processes in action potential generation [3, 13, 16] and exhibits a sigmoidal shape. In the following, we assume the same firing thresholds V_0 for all neurons function. Thus the transfer function is chosen to the Heaviside step function $S(V) = \Theta(V - V_0)$ and the system becomes binary. Few simple calculations on (1) show the existence of two stationary constant states $V_{max} = \kappa + \mu$ and $V_{min} = 0$.

Now, a transformation to the moving frame $V(x,t) = V(x - ct) = V(z)$ with the front speed c simplifies the analysis. Boundary conditions $V(z \to -\infty) = V_{max} > V_0$, $V(z \to \infty) = V_{min} < V_0$ and $V(0) = V_0$ guarantee the traveling front solutions. In addition, the condition $-v < c < v$ guarantees physically reasonable solutions consistent to previous findings [6, 28, 18]. Assuming $V(z) > V_0 \ \forall \ z < 0$ and $V(z) \leq V_0 \ \forall \ z \geq 0$ Eq. (1) yields

$$-c\frac{\partial}{\partial z}V(z) + V(z) \quad = \quad h(z) \tag{2}$$

with

$$h(z) \quad = \quad \int_{-\infty}^{\delta z} A(z - z')dz' + \int_{-\infty}^{-c\tau} F(z - z')dz' \tag{3}$$

and $\delta = c/(c - v) \ \forall \ z \geq 0$, $\delta = c/(c + v) \ \forall \ z < 0$.

Now, we examine the dependance of the front speed c from various parameters. In case of $c > 0$, solving Eq. (2) by partial integration yields divergent solutions for $z \to \infty$. However, to obtain finite solutions the sum of divergent terms g need to vanish. Following the same path of calculations in case of $c < 0$, we find divergent solutions for $z \to -\infty$. Thus non-divergent solutions $V(z)$ stipulate $g = 0$ with

$$\begin{aligned} g \quad &= \quad \kappa/2 + \mathcal{L}[F(u + |c|\tau)](0) - V_0 \\ &\mp \quad \mathcal{L}[A(u)](\frac{1}{|c|} \mp \frac{1}{v}) \mp e^{\tau}\mathcal{L}[F(u + |c|\tau)](\frac{1}{|c|}), \end{aligned} \tag{4}$$

which defines the threshold V_0 subject to the parameters. Here and in the following, $\mathcal{L}[\cdot]$ denotes the Laplace transform and the upper (lower) sign represents the case $c \geq 0$ ($c < 0$). As shall be seen in the subsequent paragraph, Eq. (4) defines the resulting front speed for fixed threshold V_0.

In a first analysis step, we neglect the feedback $F = 0$. Utilizing the relations $(\partial g/\partial v)\ dv = -g'\ dc$ and $g' = \partial g/\partial c$, we find the relation $dc/dv = -(\partial g/\partial v)/g'$. It turns out, that $\partial g/\partial v = \mathcal{L}[uA(u)](w)/v^2$ and $g' = -\mathcal{L}[uA(u)](w)/c^2$ with $w = 1/|c| \mp 1/v$. This leads to $dc/dv = c^2/v^2$ for all kernels A. That is the front speed monotonically increases with increasing transmission speed for all axonal kernels. Additionally, for $v \to \infty$, the front speed c saturates to c_0 with $V_0 - \kappa/2 = \mp\ \mathcal{L}[A](1/|c_0|)$.

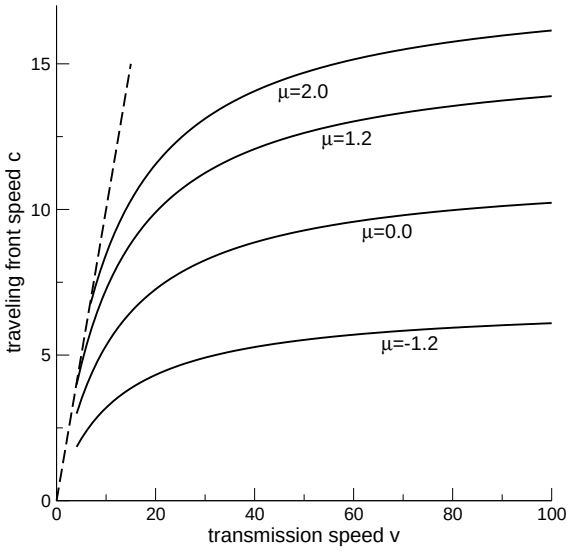

Figure 2: The front speed plotted with respect to the transmission speed for various feedback strengths for the kernels (5). The parameters are set to $a_e = 2.0,\ a_i = 2.0,\ V_0 = 0.1,\ \tau = 0.01,\ \sigma = 0.8$ and $r = 2.0$.

In order to study the case $F \neq 0$ in some detail, the analysis focus to the family of exponential kernels

$$A(z) = \frac{a_e}{2}e^{-|z|} - \frac{a_i r}{2}e^{-r|z|} \quad , \quad F(z) = \frac{\mu}{2\sigma}e^{-|z|/\sigma}, \tag{5}$$

where σ gives the spatial feedback range, a_e and a_i are excitatory and inhibitory weights and r abbreviates the ratio of excitatory and inhibitory spatial ranges (cf. [18]). For instance, in case of $a_e = a_i$, $r < 1$ and $r > 1$ corresponds to local excitation-lateral inhibition and local inhibition-lateral excitation, respectively. With these definitions Eq. (4) recasts to

$$\begin{aligned} g &= \frac{a_e}{2}\frac{v - |c|}{v - |c| + v|c|} - \frac{a_i}{2}\frac{v - |c|}{v - |c| + rv|c|} \\ &\quad + \frac{\mu}{2}\frac{\sigma}{\sigma + |c|}e^{-|c|\tau/\sigma} - V_0. \end{aligned} \tag{6}$$

We find $dc/dv = c^2/(v^2 + b\mu)$ with $b = b(|c|, v, \sigma, \tau, a_e, a_i)$. Figure 2 shows the relation of c and v for excitatory and inhibitory feedback, which is similar to results in previous studies for vanishing feedback loops (cf. [28, 9]). Further, the figure indicates a monotonic increase(decrease) of the front speed by increased excitatory(inhibitory) feedback. In order to examine this relation in some more detail, we focus to $dc/d\mu = -(\partial g/\partial \mu)/g'$. First let us take a look at the sign of g'. We find for $a_i = 0$ and $v \gg |c|$

$$\mu_c = a_e \left[\frac{1 + |c|}{\sigma + |c|}(\tau + \frac{\sigma}{\sigma + |c|})e^{-|c|\tau/\sigma}\right]^{-1}$$

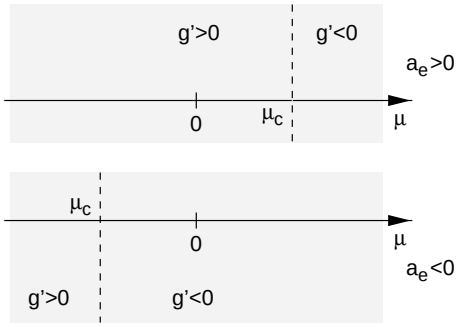

Figure 3: Sketch of the relation between μ and g'.

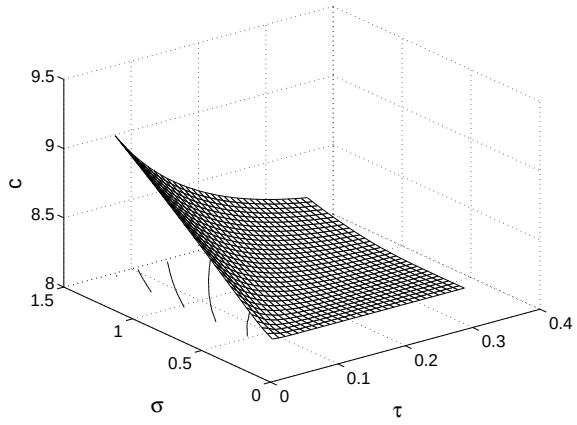

Figure 4: The front speed c with respect to the feedback range σ and the feedback delay τ for the kernels (5). Other parameters are $a_e = 2.0,\ a_i = 0.0,\ V_0 = 0.1$ and $\mu = 7.81$.

for $g' = 0$. It turns out, that excitatory fields with $a_e > 0$ yield $\mu_c > 0$ and Eq. (6) gives $\partial g/\partial \mu \geq 0$ for $\mu \geq 0$. In addition, it is $g' < 0$ for $\mu > \mu_c$ which leads to $dc/d\mu > 0$ for $\mu > \mu_c$. That is, increasing excitatory feedback in excitatory fields increases the front speed. In case of $0 < \mu < \mu_c$, it is $g' > 0$ and $dc/d\mu < 0$, i.e. increasing excitatory feedback may also reveal decreasing front speeds. Figure 3 summarizes the results and confirms Fig. 2. Inhibitory fields with $a_e < 0$ yield $\mu_c < 0$ and the resulting relations can be derived in a similar way by Fig. 3. With these results, it is straightforward to find the relation of the front speed to the feedback delay and the feedback range. It is $dc/d\tau = \mu \cdot a/g'$ and $dc/d\sigma = -\mu \cdot b/g'$ with $a(c, \sigma, \tau) > 0$ and $b(c, \sigma, \tau) > 0$. Figure 4 illustrates these relations for parameters with $g\prime < 0$. Interestingly, it is also $d\sigma/d\tau = a/b > 0$ for constant c. That is increased feedback delay times demand an increased feedback range for constant front speeds. The level lines in Fig. (4) confirms this result.

Finally, we focus to the shape of the traveling front and find for general kernels

$$\begin{aligned} V(z) &= \int_{-\infty}^{\delta z} A(z-u)du + \int_{-\infty}^{-c\tau} F(z-u)du \\ &+ \int_0^z \left((1-\delta)A((1-\delta)u) + F(u+c\tau)\right) e^{(z-u)/c} du \\ &\mp e^{z/c}\left(\mathcal{L}[A(u)](\frac{1}{|c|} \mp \frac{1}{v}) + e^{\tau}\mathcal{L}[F(u+|c|\tau)](\frac{1}{|c|})\right) \end{aligned} \tag{7}$$

Typical traveling fronts exhibit a single inflection point and approach horizontal asymptotics for $|z| \to \infty$. However, a close look at Eq. (2) indicate a sign change of dV/dz due to nonlocal feedback, i.e. local extrema of $V(z)$ may exist. Considering Eqs. (2), (7) the sufficient condition for local extrema reads

$$\begin{aligned} &\mathcal{L}[A(u)](\frac{1}{|c|} \mp \frac{1}{v}) + e^{\tau}\mathcal{L}[F(u+|c|\tau)](\frac{1}{|c|}) \\ &= \pm \int_0^{z_e} \left((1-\delta)A((1-\delta)u) + F(u+|c|\tau)\right) e^{-u/c} du \end{aligned} \tag{8}$$

.

That is the typical shape of the traveling front is changed if Eq. (8) shows real roots z_e. In addition, the type of extrema is given by the sign of

$$\frac{\partial^2 V}{\partial z^2}|_{z=z_e} = \frac{(1-\delta)}{c} A(z_e(1-\delta)) + \frac{1}{c} F(z_e + c\tau). \tag{9}$$

Now recall the implicit condition $\partial V/\partial z < 0$ at $z = 0$. This condition constraints the set of possible local extrema. For $z_e > 0$ Eq. (8) needs an even number of solutions with both positive and negative signs of $\partial^2 V/\partial z^2$ at $z = z_e$. In contrast, $z_e < 0$ facilitates an arbitrary number of extrema with at least one maximum. Figure 5 shows the novel shape by plotting $V(z)$ from Eq. (7) for appropriate parameters. Here, inhibitory feedback results to a local minimum and maximum, while excitatory feedback does show the typical shape with a steeper front. Assessing these analytical solutions numerically by inserting them to Eq. (2) reveals good accordance (not shown).

A further sufficient criterion for the occurence of local extrema is the existence of a horizontal inflection point, from which both a local minimum and local maximum grows by changing parameters. According to Eq. (9), the corresponding condition reads

$$\frac{v}{v+c} A(\frac{vz}{v+c}) = -F(z + c\tau) \tag{10}$$

It turns out that excitatory fields, i.e. $A > 0$, exhibit local extrema only in case of inhibitory feedback with $F < 0$, while $A < 0$ faciliates extrema for $F > 0$ only.

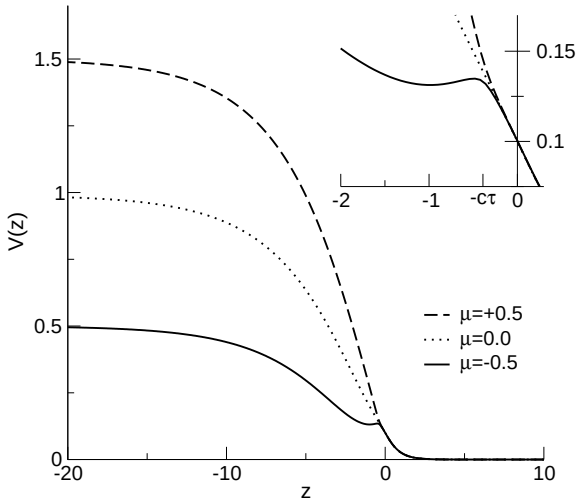

Figure 5: The traveling front for excitatory, vanishing and inhibitory nonlinear feedback for the kernels (5). Parameters are $a_e = 2.0,\ a_i = 1.0,\ r = 2.0,\ V_0 = 0.1,\ \tau = 0.1,\ \sigma = 0.1,\ v = 10.28$ and $c \approx 3.9$ for all applied values of μ.

In other words no local extrema occur in excitatory (inhibitory) fields subject to excitatory(inhibitory) feedback.

The previous sections showed the existence of traveling fronts, while no information is gained about its temporal stability towards small deviations. This problem has been attacked recently by considering Evans functions of nonlocal neural fields [36, 10]. Though this stability analysis of the proposed model might yield novel interesting results, it would exceed the major aim of this letter and we refer the reader to future work.

Summarizing, the present letter introduces nonlinear feedback to neural fields and investigates its influence to the speed of traveling fronts and its shape for general connectivity kernels. The novel front shape emerges due to nonlocal feedback of contrary sign of interaction to the field, i.e. in case of excitatory feedback in inhibitory fields and vice versa.

References

[1] M. Abeles. *Corticonics*. Cambridge University Press, 1991.

[2] S. Amari. Dynamics of pattern formation in lateral-inhibition type neural fields. *Biol. Cybernetics*, 27:77–87, 1977.

[3] D. J. Amit. *Modeling brain function: The world of attactor neural networks*. Cambridge University Press, Cambridge, 1989.

[4] A. Arieli, D. Shoham, R. Hildesheim, and A. Grinvald. Coherent spatiotemporal pattern of on-going activity revealed by real-time optical imaging

coupled with single unit recording in the cat visual cortex. *J. Neurophysiol.*, 73:2072–2093, 1995.

[5] F. M. Atay and A. Hutt. Stability and bifurcations in neural fields with axonal delay and general connectivity. *SIAM J. Appl. Math.*, in press, 2004.

[6] V. Bringuier, F. Chavane, L. Glaeser, and Y. Fregnac. Horizontal propagation of visual activity in the synaptic integration field of area 17 neurons. *Science*, 283:695–699, 1999.

[7] C. Cavada and P. S. Goldman-Rakic. Multiple visual areas in the posterior parietal cortex of primates. *Prog. Brain Res.*, 95:123–137, 1993.

[8] Z. Chen, B. Ermentrout, and B. McLeod. Traveling fronts for a class of non-local convolution differential equations. *Appl. Anal.*, 3-4:235–253, 1997.

[9] S. Coombes, G. J. Lord, and M. R. Owen. Waves and bumps in neuronal networks with axo-dendritic synaptic interactions. *Physica D*, 178:219–241, 2003.

[10] S. Coombes and M. R. Owen. Evans functions for integral neural field equations with heaviside firing rate function. *SIAM J. Appl. Dyn. Syst.*, to appear, 2004.

[11] A. Destexhe, D. Contreras, and M. Steriade. Spatiotemporal analysis of local field potentials and unit discharges in cat cerebral cortex during natural wake and sleep states. *J. Neurosc.*, 19(11):4595–4608, 1999.

[12] S. J. DiBartolo and A. T. Dorsey. Velocity selection for propagating fronts in superconductors. *Phys. Rev. Lett.*, 77:4442, 1996.

[13] B. Ermentrout. Reduction of conductance based models with slow synapses to neural nets. *Neural Computation*, 6:679–695, 1994.

[14] B. Ermentrout, J. McLeod, and J. Bryce. Existence and uniqueness of travelling waves for a neural network. *Proc. Roy. Soc.*, A 123(3):461–478, 1993.

[15] J. Fineberg and V. Steinberg. Vortex-front propagation in rayleigh-benard convection. *Phys. Rev. Lett.*, 58:1332, 1987.

[16] W. Gerstner. Time structure of the activity in neural network models. *Phys. Rev. E*, 51(1):738–758, 1995.

[17] D. Golomb and Y. Amitai. Propagating neuronal discharges in neocortical slices: computational and experimental study. *J. Neurophysiol.*, 78:1199–1211, 1997.

[18] A. Hutt, M. Bestehorn, and T. Wennekers. Pattern formation in intracortical neuronal fields. *Network: Comput. Neural Syst.*, 14:351–368, 2003.

[19] V. K. Jirsa and H. Haken. Field theory of electromagnetic brain activity. *Phys. Rev. Lett.*, 77(5):960–963, 1996.

[20] U. Kim, T. Bal, and D.A. McCormick. Spindle waves are propagating synchronized oscillations in the ferret lgnd in vitro. *J. Neurophysiol.*, 74(3):1301–1323, 1995.

[21] Y. Kuramoto. *Chemical Oscillations, Waves, and Turbulence*. Springer, Berlin, 1984.

[22] S. LeVay and S.B. Nelson. Columnar organization of the visual cortex. In J.R Cronly-Dillon, editor, *The Neural Basis of Visual Function*, pages 266–315. Macmillan, London, 1991.

[23] J.B. Levitt, D.A. Lewis, T. Yishioka, and J.S. Lund. Topography of pyramidal neuron intrinsic connections in macaque monkey prefrontal cortex (areas 9 and 46). *J. Comp. Neurol.*, 338:360–376, 1993.

[24] E. Meron. Pattern formation in excitable media. *Phys. Rep.*, 218:1, 1992.

[25] J.D. Murray. *Mathematical Biology*. Springer, Berlin, 1989.

[26] R. Osan and G. B. Ermentrout. The evolution of synaptically generated waves in one- and two-dimensional domains. *Physica D*, 163:217–235, 2002.

[27] D. Panja. Effects of fluctuations on propagating fronts. *Phys. Rep.*, 393:87–174, 2004.

[28] D. J. Pinto and G. B Ermentrout. Spatially structured activity in synaptically coupled neuronal networks: I. travelling fronts and pulses. *SIAM J. Applied Math.*, 62(1):206–225, 2001.

[29] C.Y. Saab and W.D. Willis. The cerebellum: organization, functions and its role in nociception. *Brain Res. Rev.*, 42:85–95, 2003.

[30] W. Singer. Neural synchrony: A versatile code for the definition of relations ? *Neuron*, 24:49–65, 1999.

[31] H. Spors and A. Grindvald. Spatio-temporal dynamics of odor representations in the mammalian olfactory bulb. *Neuron*, 34:301–315, 2002.

[32] M. Steriade, E. G Jones, and R. R. Llinas. *Thalamic Oscillations and Signalling*. Wiley, New York, 1990.

[33] W. van Saarloos, M. van Hecke, and R. Holyst. Front propagation into unstable and metastable states in smetic-c^* liquid crystals: linear and nonlinear marginal stability analysis. *Phys. Rev. E*, 52:1773, 1995.

[34] H. R. Wilson and J. D. Cowan. Excitatory and inhibitory interactions in localized populations of model neurons. *Biophys. J.*, 12:1–24, 1972.

[35] J. Y. Wu, L. Guan, and Y. Tsau. Propagating activation during oscillations and evoked responses in neocortical slices. *J. Neurosci.*, 19:5005–5015, 1999.

[36] L. Zhang. On stability of traveling wave solutions in synaptically coupled neuronal networks. *Differential and Integral Equations*, 16:513–536, 2003.